Arch. Mech., 50, 2, pp. 207–218, Warszawa 1998
FIFTY YEARS OF THE ARCHIVES OF MECHANICS

The gas flow through the laser-sustained plasmas

Z. SZYMAŃSKI (WARSZAWA)

MODELLING of the laser-sustained plasmas (LSP) in a forced convective flow is presented. The emphasis is put on the modelling of the flow through the region of elevated temperature. Theoretical quasi-two-dimensional and full two-dimensional models are compared. Two examples of such flow are considered. In the first, plasma is maintained by cw CO_2 laser with output power of 2 kW and burns in a stream of argon at atmospheric pressure. The results show that quasi-$2D$ model in which the axial flow is given by the relation $\varrho u = \varrho_0 u_0 (\varrho/\varrho_0)^{1/2}$, where ϱ and u are density and velocity of the cold gas, fairly well describes the LSP. The second example is the flow through the argon plasma at 1 atm attached to the surface. In this case the simplified formulae do not exist and hence only the results of the two-dimensional model are presented. They are compared with the results of calculations made for constant temperature $T = 300$ K. It has been found that the presence of the hot region considerably increases the velocity near the surface.

1. Introduction

THE FLOW through the region of elevated temperature was recently studied by several authors [1–5]. The interest in this problem is connected with the laser machining: welding, cutting or cladding. In each of these processes the stream of the shielding gas flows through the plasma that is induced by the laser radiation. The plasma is either attached to the surface of the workpiece and burns in a mixture of the shielding gas and ionized metal vapour, or is detached from the surface and burns in the shielding gas. The first situation corresponds to a jet impinging on a surface after flowing through the region of elevated temperature (plasma). The second – to a jet flowing through the plasma free-burning in the space. Both situations are considered in this paper.

The main difficulty in studying this problem theoretically lies in solving the momentum equation. The most complete description of the laser-sustained plasma (LSP) in a forced convective flow includes the equations of conservation of mass, momentum, and energy [1, 5]. The first paper in which the full $2D$ model was used to calculate laser-sustained argon plasma at 2 atm was due to JENG and KEEFER [1].

However, because of complexity of such a model, simpler models [2–4] can be sometimes favoured. In this paper free-burning laser-sustained argon plasma in a convective flow was studied using different models. The flow has been modelled either in a simplified way or by solving the full set of equations, including momentum equation. The comparison of the results shows the range of validity of simplifying assumptions.

2. Theoretical model

The flow velocity has a great influence on plasma parameters and intensity of laser radiation needed to maintain a stationary plasma. The theoretical description of experimentally observed phenomena is, however, quite complicated. The quasi-two-dimensional model [6] in which constant axial mass flux is assumed and only energy equation is solved in two dimensions, seems to be realistic only in the situation when plasma is bounded in the radial direction by walls (tube). In the case of unbounded plasma such model overestimates the influence of the flow, which is a result of $\varrho u = \text{const}$.

This problem is not serious for small velocities, few centimeters per second, which are characteristic for natural convection, because then the conduction term is much bigger than the convection term and plays the decisive role. In the case of forced convection, when inlet velocities can be of several meters per second, reliable results can only be expected from full two-dimensional model which solves the momentum equation. The solution of full set of equations consisting of energy, momentum and continuity equation is, however, quite complex. Therefore, in previous paper [4] instead of solving the full set of equations, we made certain assumption concerning the variation of the axial mass flux as a function of plasma density.

When the flow penetrates a region of increasing temperature, its behavior is similar to a flow past an obstacle. The pressure increases when approaching the hot region, the velocity decreases and most of the streamlines bypass the region of high temperature – only a relatively small part of them enter the hot region. When entering the hot region, the velocity of the gas increases with increasing temperature, due to a decrease of gas density, according to the continuity equation.

It has been shown [2, 4] that in the case when the cross-section of a hot plasma S_h is much smaller than the outer cross-section S_0 which constitutes the boundary, $S_0 \gg S_h$, we have

$$\varrho u \cong \varrho_0 u_0 \sqrt{\frac{\varrho}{\varrho_0}}. \tag{2.1}$$

Thus, when entering the low density region the mass flux is reduced by the factor $(\varrho/\varrho_0)^{1/2}$. At the other limit there is $S_h = S_0$ and

$$\varrho u = \text{const}. \tag{2.2}$$

Having defined the axial component by Eq. (2.1) (or (2.2)), the radial velocity component can be computed from the continuity equation. Equations (2.1) or (2.2) together with the equations of conservation of mass and energy constitute a quasi-$2D$ model.

In cylindrical symmetry the equations of conservation of mass, energy and momentum have the form

$$\frac{\partial \varrho}{\partial t} + \frac{1}{r}\frac{\partial(\varrho r v)}{\partial r} + \frac{\partial(\varrho u)}{\partial z} = 0, \tag{2.3}$$

$$\frac{\partial(\varrho h)}{\partial t} + \frac{\partial(\varrho r v h)}{\partial r \partial r} + \frac{\partial(\varrho h)}{\partial z} = \frac{1}{r}\frac{\partial}{\partial r}\left(\frac{r k_{\text{eff}}}{c_p}\frac{\partial h}{\partial r}\right) + \frac{\partial}{\partial z}\left(\frac{k_{\text{eff}}}{c_p}\frac{\partial h}{\partial z}\right) + \sum_i \kappa_i I_i - \Phi, \tag{2.4}$$

$$\frac{\partial(\varrho u)}{\partial t} + \frac{\partial(\varrho r v u)}{\partial r \partial r} + \frac{\partial(\varrho u u)}{\partial z} = \frac{\partial}{r \partial r}\left[\mu r\left(\frac{\partial u}{\partial r} + \frac{\partial v}{\partial z}\right)\right] + \frac{\partial}{\partial z}\left(2\frac{\mu \partial u}{\partial z}\right) - \frac{\partial p}{\partial z} - \varrho g, \tag{2.5}$$

$$\frac{\partial(\varrho v)}{\partial t} + \frac{\partial(\varrho r v v)}{\partial r \partial r} + \frac{\partial(\varrho u v)}{\partial z} = \frac{\partial}{r \partial r}\left(2\frac{r\mu \partial v}{\partial r}\right) + \frac{\partial}{\partial z}\left[\mu\left(\frac{\partial u}{\partial r} + \frac{\partial v}{\partial z}\right)\right] - \frac{\partial p}{\partial r} - \frac{2\mu v}{r^2}, \tag{2.6}$$

and the laser radiation transfer equation is given by

$$\frac{dP_i}{ds_i} = -\kappa_i P_i\,, \tag{2.7}$$

where u and v are axial and radial velocity components, respectively. h is specific enthalpy $h = h(r, z, t)$; the mass density ϱ, the specific heat at constant pressure c_p, the viscosity μ [7], the effective thermal conductivity k_{eff} [7, 8], the radiation loss function Φ [9], and the absorption coefficient κ (at 10.6 μm wavelength) depend on h only. I_i is the local laser intensity (evaluated from local laser power P_i, $I_i = P_i/\pi(r_i^2 - r_{i-1}^2)$), and s_i is the local distance along the laser ray path.

The use of the effective thermal conductivity k_{eff} is based on the assumption that the part of radiation which is absorbed in the plasma can be represented as an increase in thermal conductivity $k_{\text{rad}} + k = k_{\text{eff}}$ and included in the diffusion term.

The absorption of the 10.6 μm radiation in a plasma is described by the absorption coefficient

$$\kappa = \left[\kappa_{ei}^{ff} + \kappa_{ei}^{fb} + \kappa_{ea}\right] \times \left[1 - \exp\left(-\frac{h\nu}{kT}\right)\right], \tag{2.8}$$

where the first bracket contains the absorption due to the electron-ion inverse bremsstrahlung κ_{ei}^{ff} and photorecombination κ_{ei}^{fb} [10], and the absorption due to the electron-atom inverse bremsstrahlung κ_{ea} [11]. The second bracket contains contribution of the stimulated emission.

For small Mach numbers (say $M \leq 0.3$), the pressure changes are small and we can assume that ϱ and other thermodynamic quantities depend only on the temperature. It has also been assumed that plasma is in local thermal equilibrium (LTE). At the atmospheric pressure, the deviations from LTE are small and plasma state should be fairly close to LTE.

The relevant properties of argon used for calculations are shown in Fig. 1 in terms of temperature.

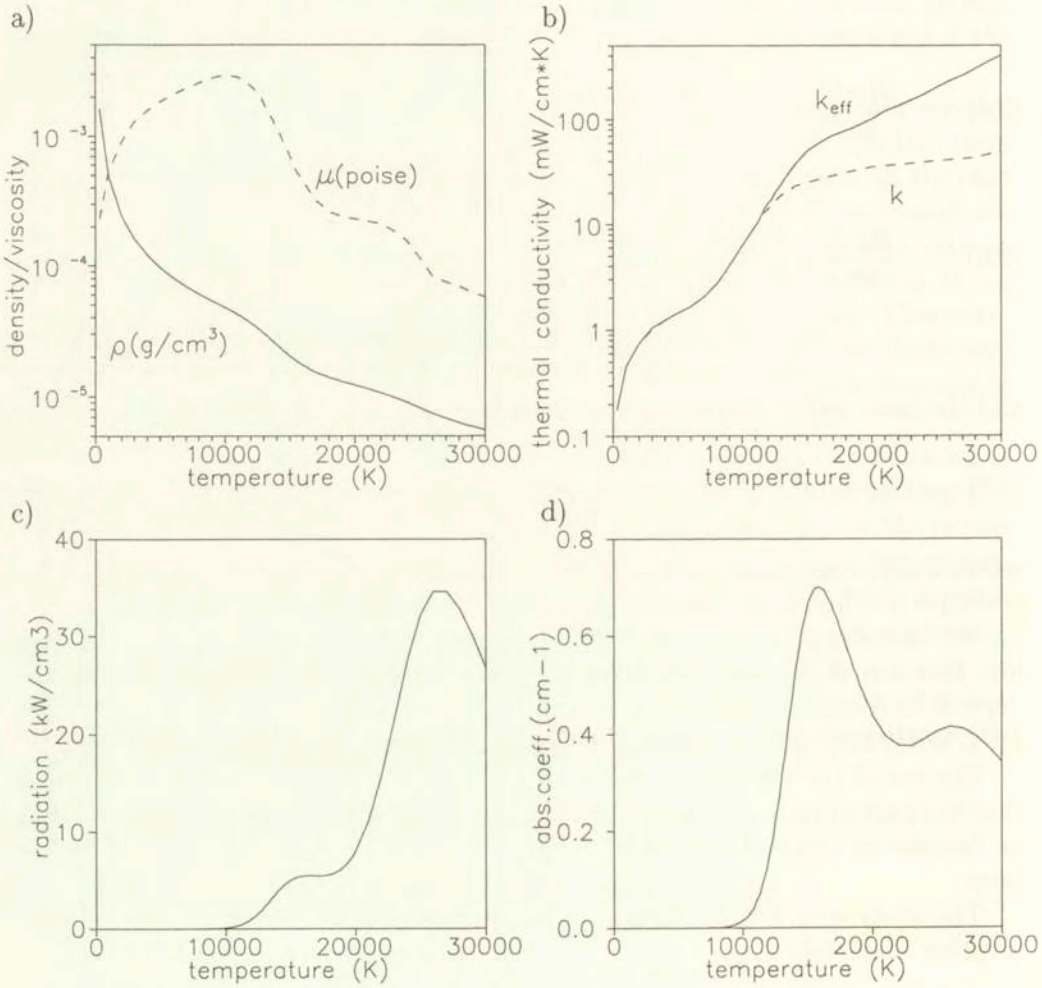

FIG. 1. Properties of argon used in the calculations in terms of temperature; a) the density and visciosity, b) the effective and pure thermal conductivity, c) the radiation power density, d) the absorption coefficient (at 10.6 μm wavelength).

The equations were solved employing the control volume method described by PATANKAR [12] and SIMPLEC algorithm [13]. In most cases a nonuniform grid

with 40 radial by 80 axial mesh was used. Reasonable results can be obtained already with a 20×40 grid. Asymptotically for large times the solution of the above set of equations leads to the stationary solution which has been used in this paper.

The laser beam was divided into 200 rays along the radial direction and the path of each ray was traced according to geometrical optics. The laser intensity distribution was assumed to be TEM_{01} mode, and exact power was ascribed to each elementary ray.

Geometrical ray tracing of the laser beam is justified for small values of the f-number because the effect of diffraction can be neglected. In our calculations the f-number, i.e. ratio of the focal length to the laser beam diameter f/D, was ~ 8.8 and hence the spherical aberration was small. Then, the geometrical optics, which does not take into account the diffraction effects, results in an unrealistically small diameter of the laser beam at the focal plane and hence, in an unrealistically high laser beam intensity in the focus spot. In this work the focus spot diameter d_f was assumed to be equal to $d_f = \Theta \times f$, where Θ is the full angle divergence of the laser beam in rad, and f is the focal length of the lens. As estimated from the measured divergence, d_f was about 0.34 mm. In numerical calculations the value of d_f was taken into account assigning the radius $r_f = d_f/2$ to the smallest computational cell. Consequently the highest laser intensity at the focal plane was $I_f = P/\pi r_f^2$ where P was the total laser power.

3. Results

3.1. Free-burning laser-sustained plasma

In the case of the free-burning laser-sustained plasma it has been assumed, according to the situation met in practice, that the laser beam and the stream of the shielding argon gas are directed vertically downwards. The boundary conditions for the system of equations were as follows. We considered discharge in infinite space but it was enough to put $T = T_B = 300\,\mathrm{K}$ at a radial distance $r = 3\,\mathrm{cm}$. For $r = 0$ the condition of symmetry requires that v and $\partial T/\partial r$ vanish. At the upstream boundary, a constant axial velocity u and uniform temperature $T = T_B$ were assigned. At the outflow boundary, $\partial T/\partial z = 0$ and $\partial(\varrho u)/\partial z = 0$ were assumed. The calculations were made for inlet velocity 5 and 2.5 m/s. The f-number was 8.8.

The temperature distributions for inlet velocity 5 m/s obtained from both quasi-$2D$ and full $2D$ theoretical models are shown in Fig. 2. The total absorption of the laser radiation in the plasma amounts to 74% while the power reradiated by the plasma is 850 W in the case of the full $2D$ model. The maximum temperature is $\sim 19500\,\mathrm{K}$. The total absorption obtained from the quasi-$2D$ model is similar but the power reradiated by the plasma is only 680 W. Because the radiation

power is a strong function of temperature, the larger radiating plasma volume at high temperatures $T > 15\,\mathrm{kK}$ encountered in the case of the full $2D$ model, results in greater radiation power.

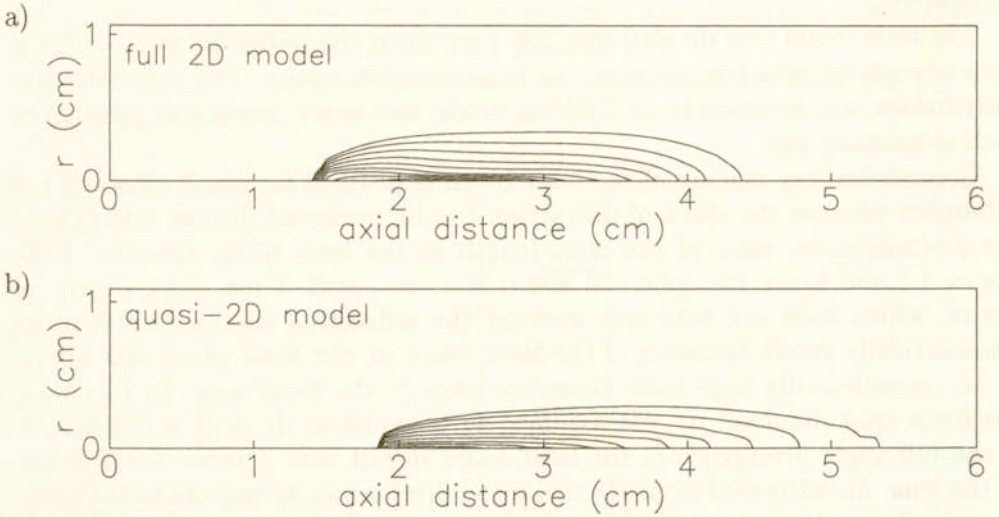

FIG. 2. Temperature distribution in a free-burning plasma; a) quasi-$2D$ model, b) full $2D$ model. Flow and laser beam direction from left to right. Outer isotherm 10000 K. Isotherms interval 1000 K. Laser power 2000 W, inlet velocity 5 m/s. Laser focal plane at $z = 2.5\,\mathrm{cm}$.

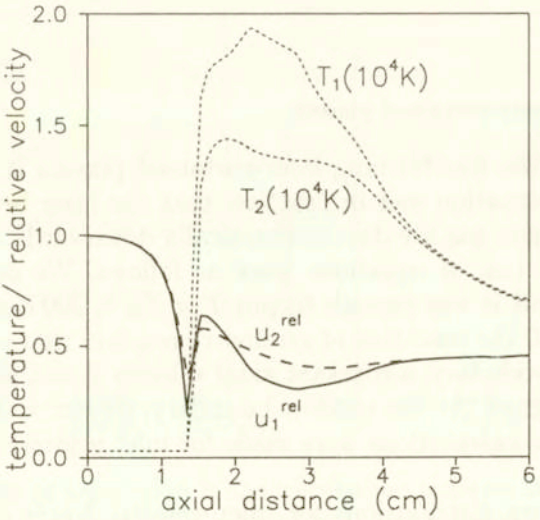

FIG. 3. Axial temperature in full $2D$ model and relative velocities $u^{\mathrm{rel}} = u(2D)/u(\text{quasi-}2D) = u/[u_0(\varrho_0/r)^{1/2}]$. Solid lines $r = 0$, dashed lines $r = 1\,\mathrm{mm}$.

Figure 3 shows the relative axial velocities $u_{\mathrm{rel}} = u_{2D}/u_{\text{quasi-}2D} = u/[u_0(\varrho_0/\varrho)^{1/2}]$ i.e., the ratio of the actual velocity calculated with the use of the full $2D$ model

and velocity used in the quasi-$2D$ model, for two different radii $r = 0$ and $r = 0.1$ cm. The axial temperatures are taken from the full $2D$ model. The worst agreement is just before the hot region. In the case of $2D$ model the velocity at the axis ($r = 0$) drops to 0.2 of the inlet value. This is the reason why in the case of the full $2D$ model, the hot plasma core is shifted upstream in comparison to the quasi-$2D$ model. In the region of high temperature, the actual velocity and velocity used in quasi-$2D$ model differ by the factor of 2. The overestimation of the axial velocity by formula (2.1) results in more elongated temperature distribution in the case of quasi-$2D$ model.

The velocity vectors and mass flux density vectors in a free-burning plasma are shown in Fig. 4. The velocity increases in the hot region but only part of axial mass flow enters the plasma core. The Reynolds number $\mathrm{Re} = \varrho u D/\mu$ is

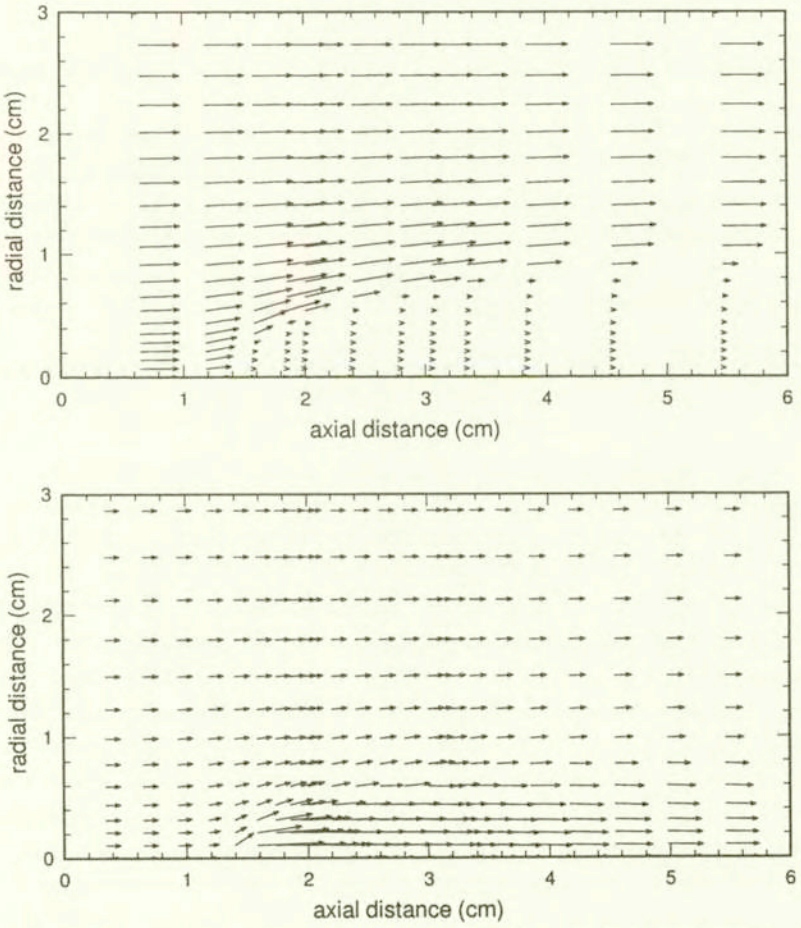

FIG. 4. Velocity vectors and mass flux density vectors in the free-burning plasma. Laser beam direction from left to right. Outer isotherm 10000 K. Isotherms interval 1000 K. Laser power 2 kW, inlet velocity 5 m/s.

~ 2000. It has been calculated using the velocity, the mass density and viscosity ahead of the hot region ($T = 300\,\mathrm{K}$), and diameter of the hot core D defined by the isotherm $T = 10000\,\mathrm{K}$.

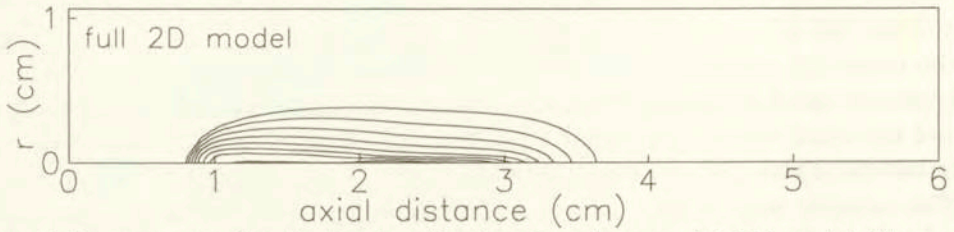

FIG. 5. Temperature distribution in a free-burning plasma – full $2D$ model. Flow and laser beam direction from left to right. Outer isotherm 10000 K. Isotherms interval 1000 K. Laser power 2000 W, inlet velocity 2.5 m/s. Laser focal plane at $z = 2.5$ cm.

The temperature distribution in a free-burning plasma (full $2D$ model) for inlet velocity 2.5 m/s is shown in Fig. 5. The decrease of the inlet velocity results in a considerable shift of the plasma relative to the focal plane in the direction of the laser beam. The total absorption of the laser radiation in the plasma amounts to 80% while the power reradiated by the plasma is 1050 W. The enhanced absorption and radiation power as compared to the results obtained for greater inlet velocity are due to different temperature profiles in both cases. The maximum temperature is $\sim 17900\,\mathrm{K}$ and is lower than that in the case of inlet velocity 5 m/s.

3.2. Impinging jet

In the case of an impinging jet it has been assumed that the stream of the shielding gas from a coaxial nozzle flows through the plasma plume attached to the surface and impinges on the workpiece. We considered the flow between two horizontal plates 1 cm apart. Again both the laser beam and the stream of the shielding argon gas are directed vertically downwards. They pass through the round hole in the upper plate and impinge on the lower one. The diameter of the hole is 6 mm. The boundary conditions were as follows. For $r = 0$ the conditions of symmetry were the same as before. At the upstream boundary, constant axial velocity u for $r \leq 3\,\mathrm{mm}$ and $u = 0$ for $r > 3\,\mathrm{mm}$ and uniform temperature $T = T_w = 300\,\mathrm{K}$ were assigned. At the surface of the lower plate both velocity components vanish. At the outflow boundary, $\partial T/\partial r = 0$ and $\partial(\varrho r v)/\partial r = 0$ were assumed. In this case the energy equation was not solved. Instead, in accordance to experimental results it has been assumed that the plasma temperature profile near the lower surface is Gaussian with the maximum temperature of 16000 K. For comparison, the calculations were also made for constant temperature $T = 300\,\mathrm{K}$. The calculations were made for inlet velocity 5 and 25 m/s.

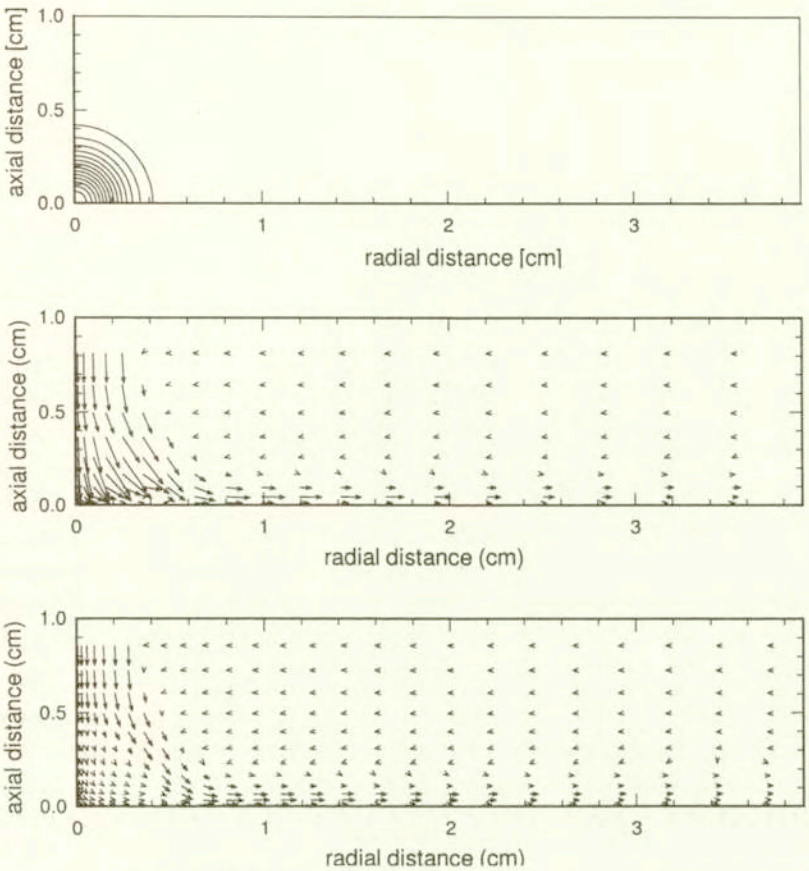

FIG. 6. Temperature distribution, velocity vectors and mass flux density vectors in an impinging jet. Outer isotherm 1000 K. Isotherms interval 2000 K. Stream inlet at the upper, left corner. Stream diameter at the inlet 6 mm, inlet velocity 5 m/s.

The results showing the temperature distribution, velocity vectors and mass flux density vectors for inlet velocity 5 m/s are shown in Fig. 6. Similarly to the case of the free-burning plasma, only part of axial mass flow enters the plasma core. Figure 7 shows the axial velocity $u(r = 0)$ profiles in terms of the axial distance for two inlet velocities 5 m/s and 25 m/s and two different temperature profiles; Gaussian (dotted line Fig. 7 a) and flat ($T = 300$ K).

It is worth noting that in the case of 25 m/s inlet velocity, the presence of the hot region increases the velocity by the factor of 7 in comparison to the solution for constant temperature $u(T_0, r, z)$ at the distance 0.1 cm from the surface. The increase depends on the inlet velocity and amounts to only 3 in the case of 5 m/s inlet velocity. In the case of the 25 m/s inlet velocity the distribution of the axial velocity is quite similar to the $u = [u(T_0, r = 0, z) \times (\varrho_0/\varrho)^{1.2}]$ where $T_0 = 300$ K (Fig. 7 b, dotted line). Such aproximation has been used in [14] where

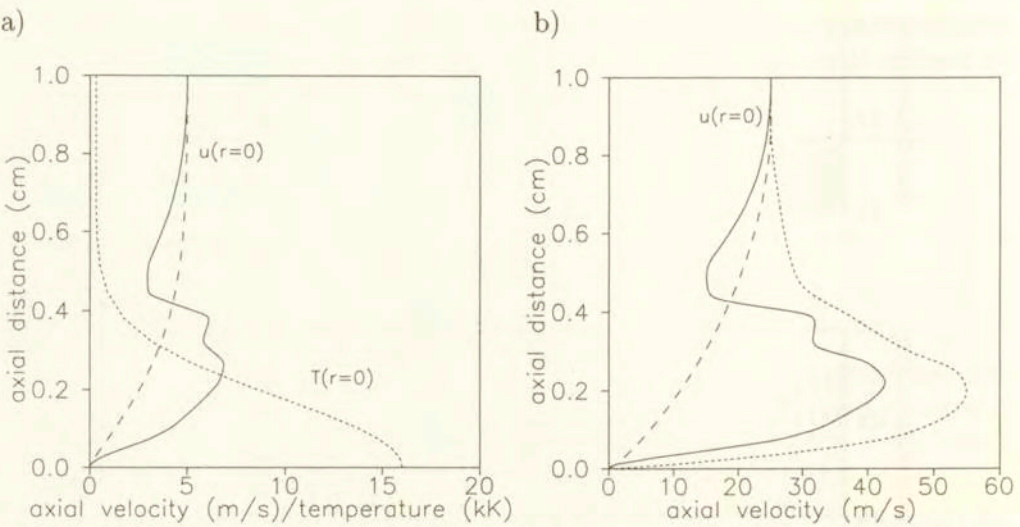

FIG. 7. Axial temperature and velocity profiles for two inlet velocities 5 m/s and 25 m/s. Solid lines: velocities calculated for the temperature profile shown in the Fig. 7 a. Dashed lines: velocities calculated for constant temperature $T_0 = 300\,\mathrm{K}$. Dotted lines: temperature (Fig. 7a), $u = [u(T_0, r = 0, z) \times (\varrho_0/\varrho)^{1/2}]$ (Fig. 7 b).

the authors used analytical solution for $u(T_0, r, z)$. However, for the inlet velocity 5 m/s, similar aproximation differs from the exact value by the factor of 3. The accuracy seems to depend on the Reynolds number and should be investigated in more detail in the future.

4. Conclusions

Numerical modelling of laser-sustained plasma in forced convective flow has been presented and two theoretical models, quasi-two-dimensional and full two-dimensional, have been compared. The results show that in the case of free-burning laser-sustained plasma, the simple formula in which the axial flow is given by the relation $\varrho u = \varrho_0 u_0 (\varrho/\varrho_0)^{1/2}$, where ϱ_0 and u_0 are the density and velocity of the cold gas, gives rough estimation of the mass flow entering the plasma. The quasi-$2D$ model overestimates the axial velocity and as a result, the plasma temperature profile is more elongated and shifted downstream in comparison with full $2D$ model.

For inlet velocities of 5 and 2.5 m/s, the absorption of the laser radiation amounts to 74% – 80% of the laser beam power, respectively, i.e. about 1500 – 1600 W in the case of 2 kW laser power. More than half of that, 850 – 1050 W is reradiated by plasma. The plasma radiation covers broad range of wavelengths, from the violet to far infrared. In the case of materials strongly reflecting laser radiation, the heating of the surface by this radiation improves thermal coupling

between the laser beam and a material. The shape of the plasma and its position with respect to the focal plane of the laser beam are slightly different for two models and the agreement with experimental data is better in the case of full $2D$ model. However, the comparison with the plasma photographs shows that the actual axial dimensions of the plasma are still about 25% smaller and at inlet velocity 5 m/s the real plasma front is shifted few mm downwards. The summation of the plasma radiation over the plasma depth showed that 95% of the radiation comes from within the isotherm of 11000 K and the dimension of this isotherm was compared with the plasma photographs. The lack of complete agreement betweem the experiment and theory is probably due to inaccuracies in the argon thermodynamic data used for the calculations. Although we checked that the calculations with the pure thermal conductivity did not change considerably the plasma shape and position of the plasma front with respect to the focal plane of the laser beam, still there could be other sources of errors like the radiation function or the absorption coefficient. Finally the lack of thermal local equilibrium can also result in different temperature profiles. This possibility, however, can only be checked by solving the two-temperature model.

The velocity distribution in the case of a jet impinging on the surface after passing through the region of high temperature, as it is in the case of the laser welding, has also been presented. In the case of the Gaussian temperature profile with the maximum temperature of 16000 K near the surface and the inlet velocity 25 m/s, the velocity increases by the factor of 7 at the distance 0.1 cm from the surface. This increase depends on the inlet velocity and most probably also on the temperature distribution near the surface. As the plasma plume influences the thermal coupling between the laser beam and the workpiece, the problem is interesting from the practical viewpoint and calls for further studies.

References

1. S-M. JENG, *Theoretical investigation of laser-sustained argon plasma*, J. Appl. Phys., **60**, 2272–2280, 1986.
2. K.G. GUSKOV, YU.P. RAIZER and S.T. SURZHIKOV, *On an observed speed of the optical discharge slow propagation* [in Russian], Kvantovaja Elektronika, **17**, 937–942, 1990.
3. Z. PERADZYŃSKI and E. ZAWISTOWSKA, *Flow in a region with large density variation*, Arch. Mech., **46**, 881–891, 1994.
4. Z. SZYMAŃSKI, Z. PERADZYŃSKI and J. KURZYNA, *Free burning laser-sustained plasma in a forced flow*, J. Appl. D: Appl. Phys., **27**, 2074–2079, 1994.
5. S.T. SURZHIKOV, *Appearace of a recirculating flow in the optical plasmotron working in the radiative regime* [in Russian], Teplofiz. Vys. Temp., **32**, 292–298, 1994.
6. R.J. GLUMB and H. KRIER, *Two-dimensional model of laser-sustained plasmas in axisymmetric flowfields*, AIAA J., **24**, 1331–1336, 1986.
7. R.S. DEVOTO, *Transport coefficients of ionized argon*, The Physics of Fluids, **165**, 616–623, 1973.
8. J. KOPAINSKY, *Strahlungstransportmechanismus und Transportkoeffizienten im Ar-Hochdruckbogen*, Z. Physik, **248**, 417–432, 1971.

9. G.I. KOZLOV, V.A. KUZNETSOV and A. MASYUKOV, *Radiative losses by argon plasma in the emissive model of a continuous optical discharge* [in Russian], Zhurnal Eksp. i Teoret. Fiziki, **66**, 954–963, 1974.
10. C.B. WHEELER and S.J. FIELDING, *Absorption of infra-red radiation as a general technique for the determination of plasma temperature*, Plasma Physics, **12**, 551–564, 1970.
11. S. GELTMAN, *Free-free radiation in electron-neutral atom collisions*, J. Quant. Spectrosc. Radiat. Transfer, **13**, 601–613, 1973.
12. S.V. PATANKAR, *Numerical heat and fluid flow*, Hemisphere, Publishing, Washington DC 1980.
13. J.P. VAN DOORMAAL and G.D. RAITHBY, *Enhancements of the SIMPLE method for predicting incompressible fluid flows*, Num. Heat Transfer, **7**, 147–163, 1984.
14. K. MAKOWSKI and Z. PERADZYŃSKI, *Modeling of a laser-sustained plasma at a metal surface*, J. Tech. Phys., **35**, 471–507, 1994.

POLISH ACADEMY OF SCIENCES
INSTITUTE OF FUNDAMENTAL TECHNOLOGICAL RESEARCH
e-mail: zszym@ippt.gov.pl

Received November 21, 1997.